

# VIBRO-ACOUSTIC ANALYSIS OF LOOSE FOUNDATION EFFECTS IN ELECTRIC MOTORS AT VARYING ROTATIONAL SPEEDS

Nikolay Yordanov<sup>1</sup>[0009-0092-1406-4754], Marin Zhilevski<sup>1</sup>[0000-0002-4545-9718], Mikho Mikhov<sup>1</sup>[0000-0002-7768-5525]

Oleg Krol<sup>2</sup>[0000-0003-0193-2750], Vladimir Sokolov<sup>2</sup>[0000-0003-0459-1824],

<sup>1</sup>Technical University of Sofia, 8 Kliment Ohridski Blvd, Sofia 1000, Bulgaria

<sup>2</sup>Volodymyr Dahl East Ukrainian National University, 17 Ioanna Pavla II str., Kyiv 01042, Ukraine

Email: [krolos@i.ua](mailto:krolos@i.ua)

**Abstract** - This study examines the impact of foundation stability on electric motor vibrations and noise fingerprint at 500–2000 RPM using continuous vibration data from vibration sensor and audio recordings from mobile phone. The aim of the research is to evaluate the effectiveness of using audio analysis as a substitute for vibration data. Another focus of the study is to compare Symmetrized Dot Pattern (SDP) with mel-spectrogram for classifying acoustic data. Both discrete (low sample count) and continuous vibration signal data are collected using vibration meter directly attached to an electric motor cage. In parallel, noise recordings are performed using mobile phone. Valuable insights in the study are provided by the observation of the relations between vibration values for displacement, velocity and acceleration in a state of loosened electric motor foundation. Employing convolutional neural networks (CNNs) like ResNet, the study achieved up to 98% accuracy in classifying operational states and faults using audio-to-image transformations (vibration data) and highlighting the potential of hybrid vibro-acoustic diagnostics for monitoring and predictive maintenance. As conclusion is found that noise audio recording together with machine learning models and image transformations can be a valuable tool for preliminary non-invasive checks, offering a cost-effective and accessible means to detect initial faults in electrical machines.

**Keywords:** Electric motor, Vibration data, Acoustic data, Fault detection, Image classification.

## 1. Introduction

Enhancing the reliability of industrial systems is crucial for maintaining high production quality [1, 2]. Fault detection in electric motors is a vital part of predictive maintenance, as these components are essential to diverse types of machinery, boosting efficiency and productivity in sectors such as manufacturing, automotive, and energy. Undetected faults, such as those caused by loose foundations or bearing wear, can lead to unexpected downtime, costly repairs, and safety hazards, underscoring the importance of robust diagnostic techniques. Timely identification of anomalies through advanced diagnostics not only enhances operational reliability but also extends the lifespan of motors, making it a priority for modern engineering practices [3, 4].

Vibration signal analysis has been firmly established as a foundational technique for condition monitoring in rotating machinery, particularly in

electric motors, where structural instabilities such as loose foundations contribute significantly to operational inefficiencies, increased wear, and potential catastrophic failures. These instabilities disrupt the normal dynamic behavior of motors, necessitating advanced diagnostic methods to mitigate risks and enhance reliability. Recent advancements in vibro-acoustic techniques have underscored the value of integrating acoustic emission signals with vibration data, offering a synergistic approach to enhance fault detection accuracy. This integration leverages sophisticated machine learning models, notably convolutional neural networks (CNNs), which have been refined to process and interpret complex datasets with improved diagnostic precision [5, 6]. The fusion of these modalities has proven instrumental in identifying subtle anomalies that might otherwise go undetected by vibration analysis alone.

Symmetrized dot pattern (SDP) transformations have emerged as a highly effective method for

visualizing and classifying both acoustic and vibration signals. By converting one-dimensional time-series data into two-dimensional images that encapsulate non-linear dynamics, SDP enables detailed pattern recognition, with applications in rotating machinery fault diagnosis achieving up to 98% accuracy when paired with advanced CNN architectures such as ResNet [7-9]. This technique has gained traction for its ability to reveal hidden correlations within vibration and acoustic data, providing a robust framework for fault characterization across varying operational conditions. Similarly, mel-spectrograms, which represent frequency content in a perceptually scaled domain, have been increasingly adopted in acoustic analysis to detect subtle variations in machinery noise. These spectrograms are often fused with vibration spectrograms, enhancing multi-class classification of operational states and faults by offering a comprehensive view of the motor's acoustic footprint [10-12]. This dual-spectrogram approach has proven particularly adept at capturing the nuanced signatures of mechanical issues, improving the granularity of diagnostic outcomes.

These innovative methodologies have demonstrated efficacy in tackling complex challenges, such as RPM-dependent resonance shifts and damping effects induced by loose mounting configurations. Acoustic signals serve as a complementary tool to traditional vibration metrics, providing additional layers of insight into the motor's health status [13-15]. The adaptability of these techniques is further enhanced by the evolution of deep learning frameworks, including ResNet and Vision Transformers, which have been optimized to manage noisy acoustic data. This optimization has significantly bolstered the robustness and reliability of fault classification, even in challenging industrial environments [16, 17]. Moreover, recent research has expanded into real-time monitoring capabilities, with hybrid acoustic-vibration frameworks showing substantial promise for predictive maintenance in industrial settings. These frameworks facilitate timely interventions by enabling continuous assessment of machinery health [18].

The deployment of edge computing for acoustic-vibration diagnostics has also gained considerable momentum, offering efficient data processing and analysis directly at the source in smart factory environments. This decentralized approach reduces latency and enhances scalability, making it a critical advancement for modern manufacturing systems [19]. Additionally, emerging studies have explored novel applications, such as fault detection in electric motors using acoustic signals and image classification techniques, leveraging SDP and CNNs to achieve high diagnostic accuracy [20]. Another significant contribution includes comparative analyses of time-frequency representations, such as

mel-spectrograms and wavelet transforms, for bearing and rotating fault diagnosis using Vision Transformers, highlighting the versatility of these methods across different fault types [21]. Collectively, these developments underscore the rapidly evolving landscape of non-invasive diagnostic techniques, capitalizing on the synergy between acoustic and vibration analyses to address the multifaceted challenges of machinery health monitoring with greater precision and efficiency.

## **2. Features of the Tested Electric Drive**

On Fig. 1 a photo is shown of the experimental setup where the tested electric drive is examined. The monitoring system includes oscilloscope, connected vibrometer of the electric motor housing and digital sound level meter.

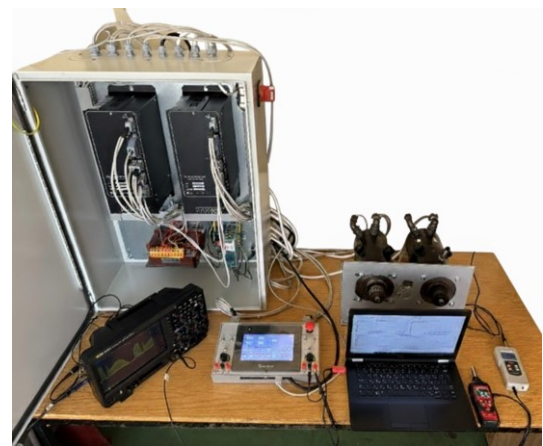


*Figure 1: Photo of the experimental setup.*

The system consists of two identical permanent-magnet direct current (DC) motors model 3PI12.12, mechanically coupled through a belt transmission, enabling controlled loading and accurate measurement of dynamic responses under different operating conditions. The nominal parameters of the motors are as follows: current - 13 A; torque - 2.7 Nm; voltage - 56 V; speed: 209.33 rad/s.

Motor control is achieved through thyristor-based converters from the 14XXX series, providing smooth regulation of both armature voltage and current. This control approach ensures high flexibility for testing various speed and torque control strategies, including transient regimes and dynamic load variations [22].

A key element of the experimental setup is the mechanical foundation on which the drive system is mounted. The base structure is made of reinforced steel and vibration-damping composite layers, ensuring high rigidity and minimal transmission of external vibrations. This guarantees that the

recorded vibration and acoustic signals originate predominantly from the tested drive system, thus improving the accuracy and reproducibility of the experimental results. A similar situation is considered in [23, 24] using the example of a machining center drive mounted on a mechanical foundation. The dynamic characteristics of the drive motor have a significant impact on the durability and operating accuracy of mechanical transmissions, predetermining the need to control this process.

The combination of controllable electrical drive parameters and a mechanically stable support platform provide a robust experimental environment for the systematic study of foundation looseness effects on the dynamic and vibro-acoustic performance of electric motors.

### 3. Methods

#### 3.1. Data Collection

On Fig. 2 a diagram with the data collection setup is shown using the mobile phone and vibrometer.

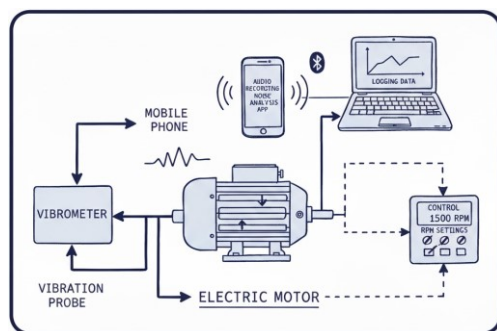


Figure 2: Data Collection Setup Diagram

The recordings are performed under different settings at 25, 50, 75 and 100 percent of the nominal parameters of the electric motor which correspond to 500, 1000, 1500 and 2000 RPM. The same settings are used to conduct recordings when foundation of the motor is loosened.

Audio recordings are made with a handheld mobile phone, held about 1 meter from the motor [25]. Each recording lasts 60 seconds and is done at the same time as vibration recordings for synchronization.

Two types of vibration data are captured at the same 60-second timeframe. Waveform Vibration data is collected using the headphones output of a vibrometer, connected to a computer's Line-In port. The headphones jack provided an analog AC voltage signal (0 to 2.0V peak full scale), reflecting the raw acceleration waveform from the vibrometer's piezoelectric accelerometer. This captured a frequency range of 10 Hz to 10 kHz.

Discrete signal vibration data is recorded using the vibration meter digital RS232/USB digital interface with sample rate between 1 and 4 seconds.

It measured average displacement, velocity, and acceleration at these intervals.

#### 3.2. Data Processing

The wave form signals (vibration and mobile phone audio) are segmented into 4-second windows with a 50% overlap, resulting in 28 segments per recording. Each 4-second segment is transformed into 2D Symmetrized Dot Pattern (SDP) images and mel-spectrograms. On Fig. 3 is shown mel-spectrogram of a noise audio subsegment from 500 RPM recording in normal state.

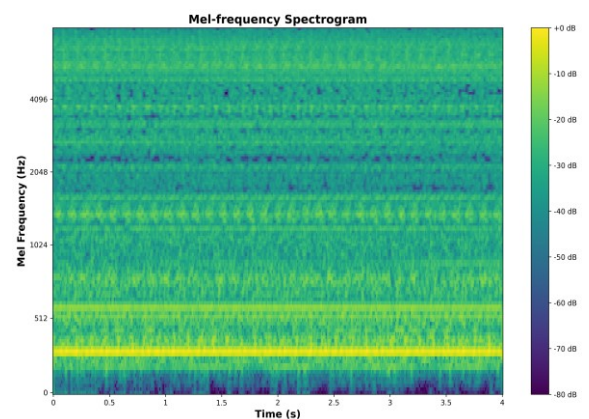


Figure 3: Mel-spectrogram of 4-second subsegment of audio noise recording at 500 RPM

On Fig. 4 SDP image representation of a noise audio recording subsegment at 500RPM in normal state is shown.

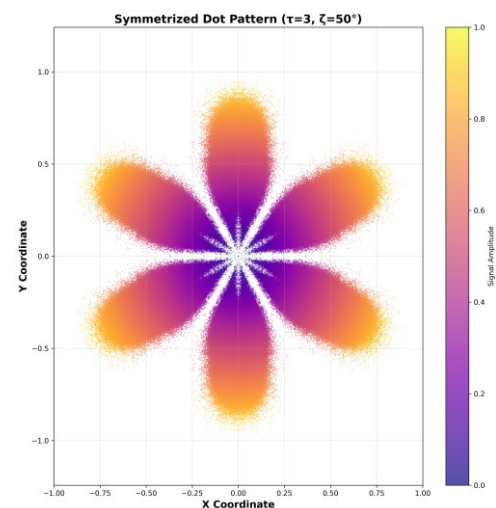


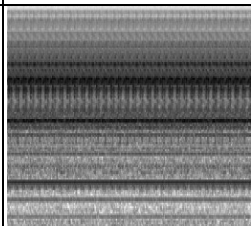
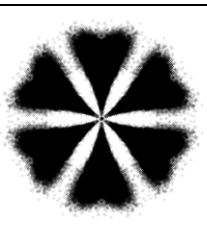
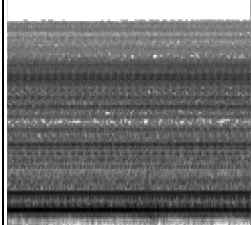
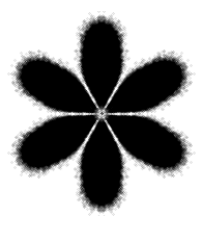
Figure 4: SDP representation of 4-seconds subsegment of audio noise recording at 500 RPM

In Table 1 are listed the images generated using the mel-spectrogram and SDP transformations of the vibration analog signal and noise audio recordings in normal state. The audio and vibration visual representation for the machine learning model training are produced in grayscale to speed up the

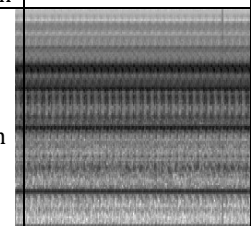
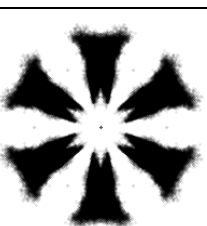
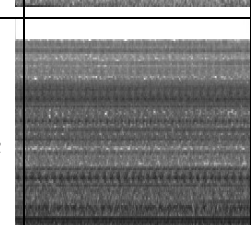
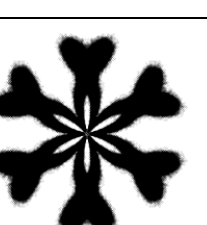
process and to minimize computational resource demands. Grayscale images internally are encoded with a single channel representing intensity values (ranging from 0 to 255), whereas RGB images utilize three channels (red, green, blue), each with its own intensity range.

This reduction from three channels to one directly impacts the dimensionality of the input data, a key factor in ML efficiency.

*Table 1. Image representation of the vibration and acoustic data 4 seconds segment at 500 RPM and normal state*

Signal Type / Transform	Mel-spectrogram	SDP
Vibration		
Acoustic		

*Table 2. Image representation of the vibration and acoustic data 4 seconds segment at 500 RPM and loosened foundation*

Signal Type / Transform	Mel-spectrogram	SDP
Vibration		
Acoustic		

In Table 2 are shown the images generated using the mel-spectrogram and SDP transformations of the vibration analog signal and noise audio recordings with loosened foundation.

### 3.3. Machine Learning Models Training and Evaluation

Convolutional neural network (CNN) models, including ResNet18, ResNet34, DenseNet121, and EfficientNetB0, are trained on the generated images derived from audio and vibration signals. The datasets are split into training and test sets using proportion 8/2. Training is conducted for 20 epochs using the cross-entropy loss function and the Adam optimizer with a learning rate set at 0.001. Losses are recorded at each epoch to monitor convergence. Convergence is observed across all models and datasets, with losses generally decreasing over epochs. For example, in the audio SDP dataset, initial losses ranged from 1.7284 (DenseNet121) to 1.9989 (ResNet34), reducing to final values between 0.3162 and 0.6790. Similar trends noted in vibration datasets, where losses approached near-zero in many cases, indicating effective learning and potential overfitting in high-performing models. Early stopping is not employed, as a fixed epoch count is used for consistency.

## 4. Results

### 4.1. Results from Vibration Discrete Signals

In Table 3 data is shown from the vibrometer. When no value is detected by the vibration meter for some of the parameters during the whole 60-second interval it is marked as N/A (not available).

*Table 3. Vibration data at different RPMs (N/A - value not available (close to 0))*

RPM	Cond.	Displacement (mm) Mean $\pm$ Std Dev	Acceleration (g) Mean $\pm$ Std Dev	Velocity (mm/s) Mean $\pm$ Std Dev
500	L	0.001	0.2923 $\pm$ 0.0277	N/N
500	N	N/N	0.5714 $\pm$ 0.0994	N/N
1000	L	0.0027 $\pm$ 0.0014	0.5571 $\pm$ 0.0756	0.0693 $\pm$ 0.0149
1000	N	0.0011 $\pm$ 0.0004	1.0929 $\pm$ 0.0917	0.1157 $\pm$ 0.0122
1500	L	0.0019 $\pm$ 0.0011	0.8929 $\pm$ 0.1269	0.1 $\pm$ 0.0104
1500	N	N/N	1.3357 $\pm$ 0.1985	0.12 $\pm$ 0.1556
2000	L	N/N	1.5 $\pm$ 0.1254	0.1527 $\pm$ 0.007
2000	N	N/N	2.1538 $\pm$ 0.2222	0.1854 $\pm$ 0.0198

For both the Loose and Normal conditions, the mean vibration levels consistently increase with RPM across all measured metrics (Acceleration and Velocity). This is the expected behavior for any rotating machinery, as higher rotational speed generates proportionally greater forces.

At 1000 RPM, the displacement in the Loose condition is approximately 2.5 times higher than in the Normal condition (0.0027 vs. 0.0011). Since displacement relates to how far the shaft or housing moves (low-frequency vibration), this finding is



consistent with physical looseness in the machine or its foundation.

Conversely, the Acceleration and Velocity metrics are significantly higher in Normal condition than in the Loose condition at all matching RPMs. This counterintuitive effect can be attributed to reduced stiffness and increased damping of the system when the foundation bolts are loosened.

## 4.2. Results from ML Training

Performance of the models is evaluated using accuracy, precision, recall, and F1-score on the test set. Classification reports and confusion matrices are generated for each model-dataset combination. Results are summarized in Tables 1 and 2, which present accuracies and macro-average F1-scores for SDP images and mel-spectrograms of both types of signals recorded. Vibration-based datasets consistently outperformed audio-based ones, with average accuracies of 0.947 (SDP) and 0.968 (Mel) for vibration compared to 0.708 (SDP) and 0.729 (Mel) for audio. This disparity highlights the superior reliability of vibration signals, which capture direct mechanical vibrations not affected by ambient noise.

In SDP transformation-based models (Table 4), perfect accuracy (1.0) is achieved by ResNet34 and EfficientNetB0 on vibration data, while audio data yielded lower results, with ResNet18 performing best at 0.766. Macro F1-scores followed a similar pattern, underscoring challenges in audio classification, particularly for classes like 1500\_L (low recall in audio).

Table 4. Comparison of model performance on SDP images

Model	Audio Accuracy	Audio Macro F1	Vibration Accuracy	Vibration Macro F1
ResNet18	0.766	0.74	0.809	0.79
ResNet34	0.702	0.68	1.000	1.00
DenseNet121	0.617	0.57	0.979	0.98
EfficientNetB0	0.745	0.74	1.000	1.00

For Mel spectrograms (Table 5), vibration again dominated, with three models reaching 1.0 accuracy, whereas audio results are mixed; EfficientNetB0 excelled at 0.979, but ResNet34 underperformed at 0.170, possibly due to instability in training losses.

Table 5. Comparison of model performance on mel-spectrogram images

Model	Audio Accuracy	Audio Macro F1	Vibration Accuracy	Vibration Macro F1
ResNet18	0.830	0.84	1.000	1.00
ResNet34	0.170	0.08	0.872	0.86
DenseNet121	0.936	0.94	1.000	1.00
EfficientNetB0	0.979	0.98	1.000	1.00

On the figures below (Fig. 5 – Fig. 8) are listed confusion matrices from the models which provided highest accuracy in the specific transformation and signal type combination.

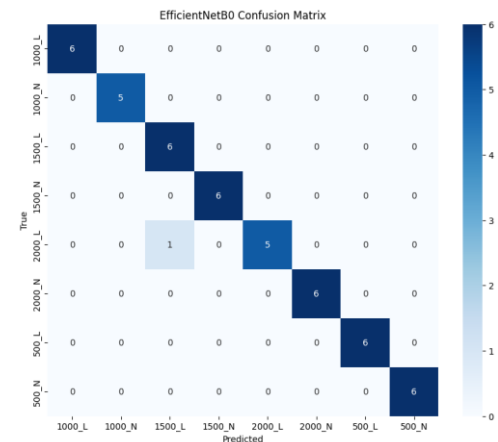


Figure 5: Confusion matrix for model with the highest accuracy trained with audio data transformed using mel-spectrograms

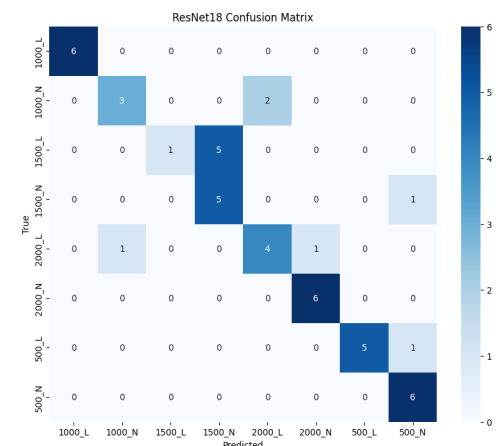


Figure 6: Confusion matrix for model with the highest accuracy trained with audio data transformed using SDP transformation

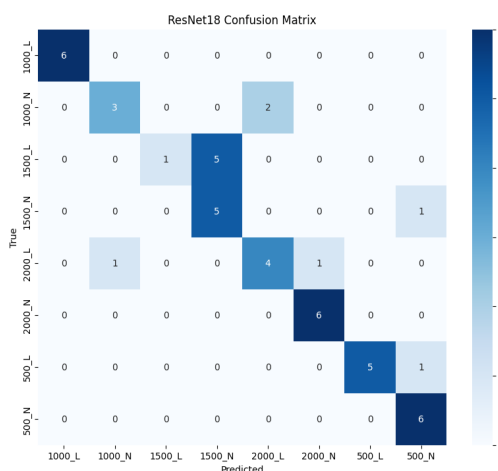


Figure 7: Confusion matrix for model with the highest accuracy trained with vibration data transformed using SDP transformation

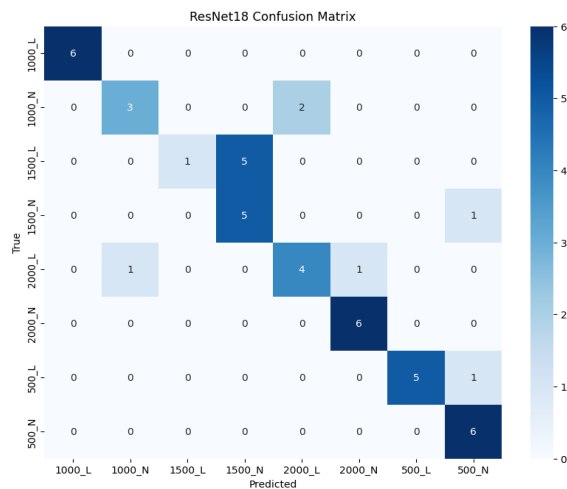


Figure 8: Confusion matrix for model with the highest accuracy trained with Audio data transformed using mel-spectrogram transformation

## 5. Conclusions

Although vibration analysis achieves nearly 100% accuracy in detecting electric motor conditions, acoustic analysis offers a viable, non-invasive alternative for preliminary fault detection, especially in restricted industrial settings.

By selecting optimal transformations (e.g., mel-spectrograms or SDP) and neural network architectures (e.g., ResNet), acoustic diagnostic accuracy can be significantly improved. Loose foundations counterintuitively reduce acceleration and velocity while increasing displacement due to lower stiffness and damping. Mel-spectrograms outperform SDP in capturing these variations, due to their enhanced frequency representation.

Future work may explore hybrid vibration-acoustic models and denoising techniques, such as wavelet transforms, to enhance robustness. Additionally, research is planned to integrate audio noise analysis with thermal imaging camera data to assess the enhanced potential of this multimodal approach for non-invasive electric motor diagnostics, potentially uncovering correlations between thermal and acoustic anomalies. It will also explore advanced transformations like wavelet and Hilbert-Huang transforms, along with innovative models such as Transformer-based architectures and Graph Neural Networks, to boost fault detection accuracy and robustness across varied conditions.

## Acknowledgement

This research was funded by the Research and Development Sector at the Technical University of Sofia, Bulgaria under Project No. 242PD0002-08/2024.

## References

- [1] Yakovenko, I., Permyakov, A., Dobrotvorskiy, S., Basova Y., Kotliar, A., & Zinchenko, A. (2023). Prospects for the development of process equipment in aggregate-modular design for sustainable mechanical engineering. *International Journal of Mechatronics and Applied Mechanics: Issue 13*, (pp. 145–156). <https://dx.doi.org/10.17683/ijomam/issue13.18>
- [2] Basova, Y., Dobrotvorskiy, S., Balog, M., Iakovets, A., Amine, C.M., & Zinchenko, A. (2023). Increasing SME Supply Chain Resilience in the Face of Rapidly Changing Demand with 3D Model Visualisation. *International Journal of Mechatronics and Applied Mechanics*, 14, 35–47. <https://doi.org/10.17683/ijomam/issue14.5>
- [3] Shubita, R., Alsadeh, A. & Khater, I. (2023). Fault detection in rotating machinery based on sound signal using edge machine learning. *IEEE Access*, 11, 6665–6672. <https://doi.org/10.1109/ACCESS.2023.3237074>
- [4] ElAraby, W., Madian, A. & Saad, M. (2025). Fault diagnosis for rotating machinery based on deep learning. *Noise & Vibration Worldwide*, 56, 400–421. <https://doi.org/10.1177/09574565251348863>
- [5] Wang, X., Mao, D., & Li, X. (2021). Bearing fault diagnosis based on vibro-acoustic data fusion and 1D-CNN network. *Measurement*, 173, 108518. <https://doi.org/10.1016/j.measurement.2020.108518>
- [6] Ertarğın, M., Yildirim, Ö., & Orhan, A. (2024). Mechanical and electrical faults detection in induction motor across multiple sensors with CNN-LSTM deep learning model. *Electrical Engineering*, 106, 6941–6951. <https://doi.org/10.1007/s00202-024-02420-w>
- [7] Cui, W., Meng, G., Gou, T., Wang, A., Xiao, R., & Zhang, X. (2022). Intelligent rolling bearing fault diagnosis method using symmetrized dot pattern images and CBAM-DRN. *Sensors*, 22, 9954. <https://doi.org/10.3390/s22249954>
- [8] Wang, H., Xu, J., Yan, R., & Gao, R. (2020). A New Intelligent Bearing Fault Diagnosis Method Using SDP Representation and SE-CNN. *IEEE Transactions on Instrumentation and Measurement*, 69(5), 2377–2389. <https://doi.org/10.1109/TIM.2019.2956332>
- [9] Diwakar, A., & Manivannan, P. (2019). Symmetrised dot pattern technique for fault diagnosis in a spur gear assembly using vibration signals. *IOP Conference Series: Materials Science and Engineering*, 561, 012079. <https://doi.org/10.1088/1757-899X/561/1/012079>
- [10] Shaikh, K., Jawarkar, N., Ahmed, V., & Charniya, N. (2025). Audio anomaly detection in industrial machines using inverse-Mel scale spectrograms. *Systems and Soft Computing*, 7, 200398. <https://doi.org/10.1016/j.sasc.2025.200398>

- [11] Bin Saharom, A., & Ehara, F. (2024). Comparative Analysis of MFCC and Mel-Spectrogram Features in Pump Fault Detection Using Autoencoder. *2024 2nd International Conference on Computer Graphics and Image Processing (CGIP)*. IEEE. 124–128. <https://doi.org/10.1109/CGIP62525.2024.00030>
- [12] Mian, T., Choudhary, A., Fatima, S., & Panigrahi, B. (2023). Mel-spectrogram based Approach for Fault Detection in Ball Bearing using Convolutional Neural Network. *ICECC '23*, 283–289. <https://doi.org/10.1145/3592307.3592352>
- [13] de Walque, C., & Jamaluddin, R. (2023). Vibro-acoustic Study of a Full Vehicle Excited by an Electric Motor: Structure-borne and Air-borne Noise Comparison. *SAE Technical Paper 2023-01-1112*. <https://doi.org/10.4271/2023-01-1112>
- [14] Król, E., Maciążek, M., & Wolnik, T. (2023). Review of Vibroacoustic Analysis Methods of Electric Vehicles Motors. *Energies*, 16, 2041. <https://doi.org/10.3390/en16042041>
- [15] Yang, C., Gan, X., Peng, A., & Yuan, X. (2023). ResNet Based on Multi-Feature Attention Mechanism for Sound Classification in Noisy Environments. *Sustainability*, 15, 10762. <https://doi.org/10.3390/su151410762>
- [16] Rashed, A., Abdulazeem, Y., Farrag, T., Bamaqa, A., Almaliki, M., Badawy, M., & Elhosseini, M. (2025). Toward Inclusive Smart Cities: Sound-Based Vehicle Diagnostics, Emergency Signal Recognition, and Beyond. *Machines*, 13, 258. <https://doi.org/10.3390/machines13040258>
- [17] Yang, D., Lv, Y., Yuan, R., Yang, K., & Zhong, H. (2022). A novel vibro-acoustic fault diagnosis method of rolling bearings via entropy-weighted nuisance attribute projection and orthogonal locality preserving projections under various operating conditions. *Appl. Acoust.*, 196, 108889. <https://doi.org/10.1016/j.apacoust.2022.108889>
- [18] Tiboni, M., Remino, C., Bussola, R., & Amici, C. (2022). A Review on Vibration-Based Condition Monitoring of Rotating Machinery. *Appl. Sci.*, 12, 972. <https://doi.org/10.3390/app12030972>
- [19] Romanssini, M., de Aguirre, P.; Compassi-Severo, L., & Girardi, A. (2023). A Review on Vibration Monitoring Techniques for Predictive Maintenance of Rotating Machinery. *Eng*, 4(3), 1797-1817. <https://doi.org/10.3390/eng4030102>
- [20] Ertarğın, M., Yordanov, N., & Zhilevski, M. (2025). Health Status Classification of Electric Motors Using CNN-Based Models and SDP Images Under Varying Noise Conditions. Presented at: *11th World Congress on Electrical Engineering and Computer Systems and Science*, Paris, France. <https://doi.org/10.11159/eee25.107>
- [21] Orhan, A., Yordanov, N., Ertarğın, M., Zhilevski, M., & Mikhov, M. (2025). A Comparative Study of Time-Frequency Representations for Bearing and Rotating Fault Diagnosis Using Vision Transformer. *Machines*, 13(8), 737. <https://doi.org/10.3390/machines13080737>
- [22] Faulhaber, 2025, [online] Available: <https://ell-bg.com/en/products/servo-drives/12-13-14xxx-series-digital-thyristor-converters-for-controlling-permanent-magnet-dc-motors/>
- [23] Krol, O. (2021). Modeling of Worm Gear Design with Non-clearance Engagement. In: A.A. Radionov, & V.R. Gasiyarov (Eds.) *Proceedings of the 6th International Conference on Industrial Engineering (ICIE 2020)*. LNME (pp. 36–46). Springer, Cham. [https://doi.org/10.1007/978-3-030-54814-8\\_5](https://doi.org/10.1007/978-3-030-54814-8_5)
- [24] Shevchenko, S., Mukhovaty, A., & Krol, O. (2021). Modification of Two-Stage Coaxial Gearbox. In: A.A. Radionov, & V.R. Gasiyarov, (Eds.) *Proceedings of the 6th International Conference on Industrial Engineering (ICIE 2020)* (pp. 28–35). Springer, Cham. [https://doi.org/10.1007/978-3-030-54814-8\\_4](https://doi.org/10.1007/978-3-030-54814-8_4)
- [25] Jombo, G., & Zhang, Y. (2023). Acoustic-Based Machine Condition Monitoring—Methods and Challenges, *Eng*, 4(1), 47-79. <https://doi.org/10.3390/eng4010004>